

E-CLIP: Towards Label-efficient Event-based Open-world Understanding by CLIP

Jiazhou Zhou*, Xu Zheng*, *Student Member, IEEE*, Yuanhuiyi Lyu, Lin Wang†, *Member, IEEE*

Abstract—Contrasting Language-image pertaining (CLIP) has recently shown promising open-world and few-shot performance on 2D image-based recognition tasks. However, the transferred capability of CLIP to the novel event camera data still remains under-explored to date. In particular, due to the distinct modality gap with the image-text data and the lack of large-scale datasets, achieving this goal is non-trivial and thus requires significant research innovation. In this paper, we propose **E-CLIP**, a novel and effective framework that unleashes the potential of CLIP for event-based recognition to compensate for the lack of large-scale event-based datasets. Our work addresses two crucial challenges: 1) how to generalize CLIP’s visual encoder to event data while fully leveraging events’ unique properties, *e.g.*, sparsity and high temporal resolution; 2) how to effectively align the multi-modal embeddings, *i.e.*, image, text, and events. To this end, we first introduce a novel event encoder that subtly models the temporal information from events and meanwhile generates event prompts for modality bridging. We then design a text encoder that generates content prompts and utilizes hybrid text prompts to enhance the E-CLIP’s generalization ability across diverse datasets. With the proposed event encoder, text encoder, and original image encoder, a novel Hierarchical Triple Contrastive Alignment (HTCA) module is introduced to jointly optimize the correlation and enable efficient knowledge transfer among the three modalities. We evaluate various settings, including fine-tuning, zero-shot, and few-shot on three benchmarks and our E-CLIP achieves new state-of-art accuracy compared with the previous methods, such as on N-Caltech101 (+3.94% and +4.62%) and N-Imagenet(+4.77% and +2.92%) with fine-tuning and 20-shot settings respectively. Moreover, our E-CLIP can be flexibly extended to the event retrieval task using text or image queries, showing plausible performance. Project homepage: <https://vlislab22.github.io/ECLIP/>.

Index Terms—Event-based Recognition, CLIP, Open-world, Few-shot Learning, Event Retrieval

arXiv:2308.03135v2 [cs.CV] 10 Sep 2023

1 INTRODUCTION

Event cameras are bio-inspired sensors [1], [2] that have recently received much attention in the computer vision and robotics community for their distinct merits, such as high temporal resolution and no motion blur. Event cameras perceive the per-pixel brightness changes asynchronously and output event streams, encoding the time, pixel location, and polarity of intensity changes. This distinct feature has sparked many research endeavors targeted at event cameras, and recently deep neural networks (DNNs) have been applied to event-based vision, showing significant performance gains for many tasks, such as object recognition [3], [4], [5], [6], [7], [8], [9]. Event cameras pose superior performance in capturing objects in dynamic environments; however, learning high-performance DNNs for event data is often impeded by the asynchronous nature of events and the challenge of obtaining high-quality and large-scale labeled datasets [1], [2], [10]. Moreover, in real-world scenarios, DNN model failures may occur when encountering event data with new categories not present in the training set. Nonetheless, retraining large models for each new category is impractical, making it necessary to explore zero-shot and few-shot recognition pipelines for event cameras.

Recently, vision-language models (VLMs), *e.g.*, CLIP [11], have shown promising open-world performance on the 2D image-

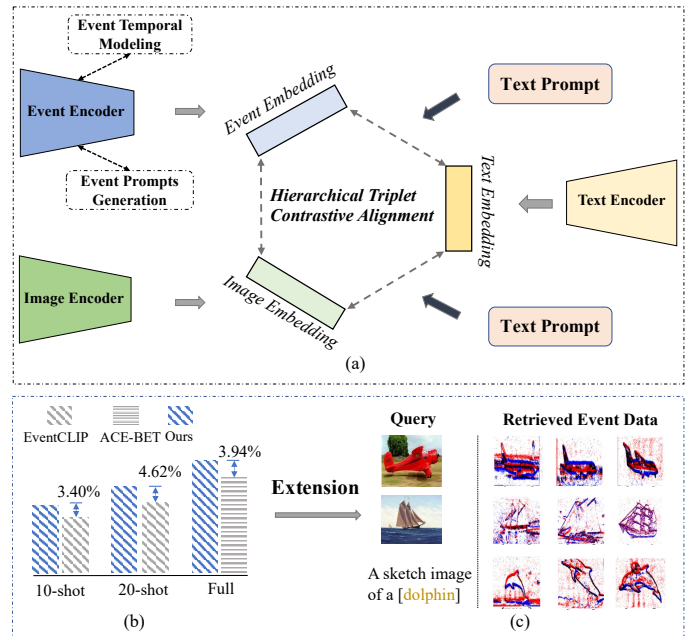


Fig. 1. (a) **Overview of our E-CLIP framework**, which extracts the high temporal and sparse spatial information from events via the proposed event encoder and aligns events, image, and text embeddings in the unified feature space with a novel hierarchical Triple contrastive alignment module. (b) The event recognition performance gains of our E-CLIP against the previous best model, including EventCLIP [10] for few-shot performance and ACE-BET [9] for fine-tuning performance on the N-Caltech101 dataset. (c) Our E-CLIP framework can be flexibly extended to event data retrieval.

- J. Zhou, X. Zheng, Y. Lyu are with the AI Thrust, HKUST(GZ), Guangzhou, China. E-mail: zhengxu128@gmail.com, {jiazhouzhou, yuanhuiyilyu}@hkust-gz.edu.cn
- L. Wang is with the AI Thrust, HKUST(GZ), Guangzhou, and Dept. of Computer Science and Engineering, HKUST, Hong Kong SAR, China. E-mail: linwang@ust.hk

Manuscript received April 19, 2022; revised August 26, 2022.
(* Equal contribution, † Corresponding author: Lin Wang)

based recognition tasks. Benefiting from large-scale training data (more than 400M image-text pairs), CLIP can serve as the pre-trained model and be transferred to other visual data, *e.g.*, video [12], [13], [14] and depth [15], under the few-shot setting.

Despite their success, the transferred capacity of CLIP to the novel event data still remains under-explored. In particular, event streams are asynchronous, sparse, and with high-temporal resolution; therefore, treating events as images and directly applying the image encoder of CLIP [10] result in significant spatial-temporal information loss, thus leading to performance degradation, as demonstrated in Tab. 2. Intuitively, we ask a question: *how to transfer the pre-trained CLIP to the event data and achieve open-world few-shot recognition performance while considering its asynchronous feature and the distinct modality shift from the image and text data?* To this end, we strive to address two crucial challenges. **1)** how to generalize CLIP’s original visual encoder to the event data while fully leveraging events’ unique properties, *e.g.*, sparsity and high temporal resolution. That is, the distinct modality discrepancy of event data, compared with the canonical images, makes it difficult to directly extract the spatial-temporal features using CLIP’s original visual encoders. **2)** how to effectively align the multi-modal embeddings, *i.e.*, image, text, and event. The significant modality gap between these modalities poses obstacles to reliable and effective feature alignments.

In this paper, we propose **E-CLIP**, a novel framework that unleashes the potential of CLIP for event-based recognition tasks to compensate for the lack of large-scale event-based datasets. Our E-CLIP consists of an event encoder, a text encoder, and the CLIP image encoder, as illustrated in Fig. 1 (b). Our method enjoys three key technical breakthroughs. Firstly, we introduce an event encoder to address the challenge of generalizing CLIP’s original visual encoder to the event data (Sec. 4.2.1). The event encoder incorporates event temporal modeling and event prompts generation to better exploit events’ unique properties, such as sparsity and high temporal resolution. Specifically, the event temporal modeling enables temporal information exchange between event frames, while the generated event prompts are used to capture the spatial-temporal information of raw events. To better align text with events, we introduce a new text encoder in our E-CLIP, building upon the basic text encoder in CLIP (Sec. 4.2.2). The text encoder generates content prompts to improve the fine-tuning performance with a lightweight MLP network and incorporates hybrid text prompts —combining hand-crafted and learnable prompts —to enhance the generalization across diverse datasets. Moreover, we introduce an additional loss function to ensure consistency between the hand-crafted and learnable prompts.

To tackle the second challenge, we propose a Hierarchical Triple Contrastive Alignment (HTCA) module to align the multi-modal embeddings, *i.e.*, event, image, and text in a unified feature space (Sec. 4.2.3). Concretely, it conducts multi-modal triple feature alignment, which jointly aligns the texts, events, and images by minimizing the contrastive loss between each two of them. Meanwhile, it imposes the semantic feature alignment to keep the semantic consistency between events and images. In a nutshell, with the HTCA module, we can effectively bridge the modality gap and facilitate efficient knowledge transfer among the three encoders.

We conduct extensive experiments to evaluate our E-CLIP framework on three event-based recognition benchmarks: N-Caltech101, N-MNIST, and N-ImageNet, covering fine-tuning, zero-shot, and few-shot settings. The experimental results demon-

strate that our E-CLIP significantly outperforms the existing methods by a large margin (Fig. 1 (b)). Additionally, we demonstrate that our framework can be extended to the application of E-CLIP to the event retrieval task by utilizing both text and image queries, which further spotlights E-CLIP’s transferability and versatility.

In summary, our main contributions are as follows: **(I)** We propose a novel E-CLIP framework that unleashes the potential of CLIP for event-based recognition to compensate for the lack of large-scale datasets. **(II)** We propose a novel event encoder and a text encoder to harness properties of events (*e.g.*, high temporal resolution) and to enhance the E-CLIP’s generalization ability, respectively. **(III)** We propose a novel Hierarchical Triple Contrastive Alignment (HTCA) module that jointly optimizes the correlation alignment among three modalities. **(IV)** We demonstrate that our E-CLIP outperforms existing methods by a significant margin in both fine-tuning and few-shot settings on three event recognition benchmarks. As a penitential, our E-CLIP can also be freely extended to the event retrieval task when employing text or image queries.

2 RELATED WORKS

Vision-language Models (VLMs). VLMs have attracted increasing attention in recent years [16], [17] due to their potential transferring ability to various modalities, where well-aligned image-text embedding is the focal point compared with the single image information. As a pioneering work, Radford *et al.* proposed a large-scale pre-trained model, called CLIP [11], that employs contrastive learning objectives on image-text pairs and accomplishes remarkable zero-shot classification performance on more than 30 datasets. Motivated by it, a number of subsequent works have associated the original image and text modalities with other modality data, such as audio [18], 3D point clouds [17], [19], [20], [21], video [12], [13], [14], and depth [15]. In summary, these methods can be divided into three types: 1) The ‘single-encoder’ framework that utilizes the frozen CLIP visual encoder as the backbone of the additional modality encoder [22], [23]; 2) The ‘dual-encoder’ framework, which is made up by the CLIP’s text encoder and the fine-tuned CLIP’s visual encoder for the added modality embedding [12], [13], [14], [15], [19], [24]; 3) The ‘triple-encoder’ framework consisting of the CLIP’s text and visual encoders in addition to a brand-new encoder employed specifically for additional modality embedding [18], [20], [21].

However, there are few attempts on aligning the event modality with the image and text features simultaneously via the CLIP model. One concurrent work to ours is EventCLIP [10], which exploits the gray-scale event frame as the intermediate representation of event data and utilizes the CLIP visual encoder for event embedding. Our share three key technical differences with EventCLIP in that: 1) EventCLIP utilizes the CLIP’s image encoder to process event data, while our E-CLIP incorporates a specialized event encoder; 2) EventCLIP refines event embeddings to be aligned with the text embedding, whereas our E-CLIP employs triple contrastive alignment among event, image, and text modalities; 3) EventCLIP solely evaluates on the object recognition task, while our E-CLIP additionally demonstrates the effectiveness in the event retrieval task using both text and image queries.

Prompt Learning for VLMs. Prompt learning plays a pivotal role in harnessing the power of large-scale VLMs [16], [17]. Existing research primarily concentrates on crafting prompts for the VLMs, considering both the vision and language modalities.

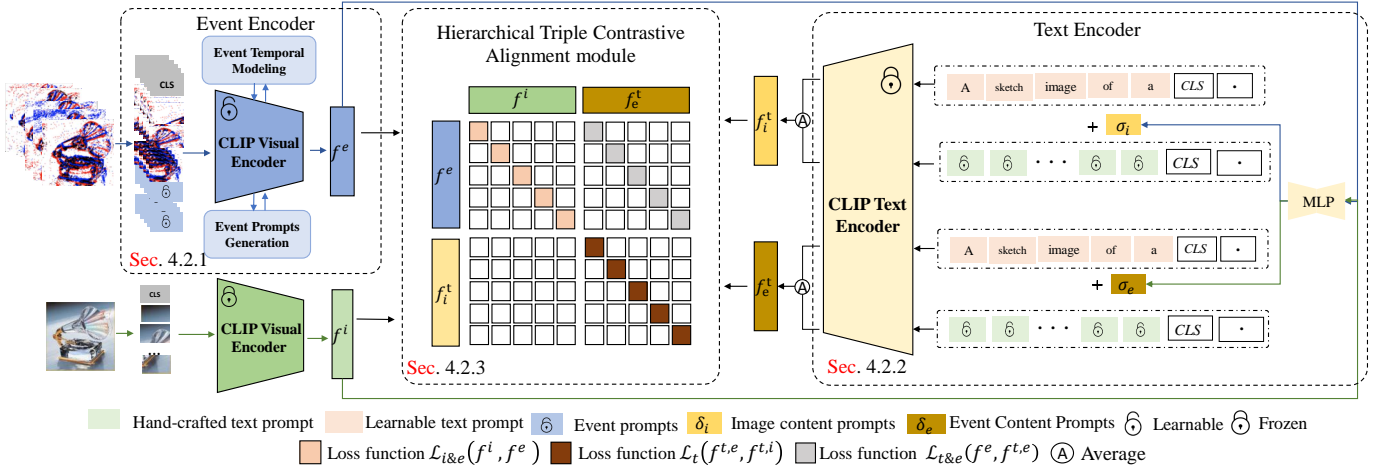


Fig. 2. **Overall framework of our proposed E-CLIP.** It consists of three encoders: 1) the event encoder which is responsible for extracting dense temporal and sparse spatial information from events and bridging the modality gap to generate the event embeddings f^e ; 2) the original CLIP’s image encoder which is used to obtain powerful and semantically aligned image embeddings f^i ; 3) the text encoder that incorporates the event and image content and pre-trained generalizing knowledge from CLIP to generate the text embeddings f_e^t, f_i^t . These three encoders take the event data, paired RGB images, and category name (text) as inputs and output event embeddings f^e , image embeddings f^i , event content added text embeddings f_e^t , and image content added text embeddings f_i^t . Finally, our Hierarchical Triple Contrastive Alignment (HTCA) module jointly optimizes the correlation among the three distinct modalities, forming a unified embedding space among image, text, and event.

Text prompts are designed to activate specific capabilities of pre-trained VLMs by the manually designed templates and learnable embeddings [11], [25], [26], [27]. These prompts guide VLMs in cross-modal understanding, achieving promising results on various tasks [28], [29], [30], [31], [32]. Visual prompts tuning injects a small number of learnable parameters into input space [33], which can enhance the performance of the visual module in VLMs [34], [35], [36] and enable rapid adaptation to downstream tasks [37], [38]. Compared to text prompts, visual prompts can be presented in various forms, such as bounding boxes [34], [39], colored blocks [40], positions [41] and points [42], providing greater flexibility to visual prompts. In our E-CLIP, we design specific event prompts based on text prompts and visual prompts to assist the model in learning the features of event data.

Event-based Recognition. Event cameras show distinct advantages such as high-temporal resolution, low latency, and very high dynamic range, making them suitable for real-time onboard object recognition in various applications, such as autonomous vehicles, and mobile systems [1]. However, the distinct imaging paradigms shift poses challenges in directly applying DNNs to learn from event data. For this reason, various methods [1], [2], [4], [5], [7], [8], [9], [43], [44], [45], [46], [47], [48] have been proposed. However, learning high-performance DNNs for event data is challenging due to the asynchronous nature of events and the lack of large-scale labeled datasets [1]. DNN model failures can occur when encountering event data with new categories not in the training set. As retraining large models for each new category is impractical, there is a need to explore zero-shot and few-shot recognition pipelines for event cameras. Intuitively, we propose E-CLIP with novel event and text encoders, buttressed by a triple contrastive alignment module, to effectively unleash the potential of CLIP to event-based recognition.

3 PRELIMINARY OF CLIP

The Contrastive Language-Image Pre-training (CLIP) [11] model is a prominent vision-language model that combines an image encoder (ViT [49] or ResNet [50]), with a text encoder based on the Transformer [51] architecture. CLIP focuses on generating

visual and text embeddings and employs a contrastive loss to align these embeddings in a unified feature space. Notably, CLIP’s exceptional transferability is attributed to its pretraining on a large-scale dataset of more than four million image-text pairs.

For CLIP-based recognition, it usually employs a simple yet efficient method that takes N hand-crafted prompts like ‘a photo of a [cls]’ as the input for the text encoder to obtain the D -dimensional textual embedding $f^t \in \mathbb{R}^{N \times D}$, where [cls] is the class name and N is the number of classes of the downstream dataset. Meanwhile, for a given image, the visual embedding $f^i \in \mathbb{R}^{1 \times D}$ is obtained by the visual encoder. Then, the recognition logits $p \in \mathbb{R}^N$ can be obtained by calculating the similarity of text and visual embeddings by multiplication:

$$p = \text{Softmax}(f^i(f^t)^T), \quad (1)$$

where $\text{Softmax}(\cdot)$ denotes the Softmax function and p represents the predicted probability of the N classes. Finally, the highest scores of the logits p is regarded as the final prediction P :

$$P = \arg \max_{i \in \mathcal{N}} p_i \quad (2)$$

Recent works have demonstrated that VLMs’ unified image-text representation space can be extended to other modalities, such as audio [18], point clouds [17], [19], [20], [21], videos [12], [13], [14], and depth [15]. Among these works, CLIP is mostly considered due to its public accessibility and prominence in the literature. Consequently, it is natural for us to question *whether the remarkable capability of CLIP can also be transferred to the asynchronous event-based vision*. However, addressing the modality disparity among events, image, and text data is nontrivial. Firstly, how to efficiently extract features from event data by considering the distinct modality shift. In this regard, it is crucial to design a tailored event encoder, which can fully leverage events’ unique properties, such as high temporal information and sparsity. Secondly, it’s still an open question to bridge the modality gap among the three distinct modalities and effectively align the multi-modal embeddings, *i.e.*, image, text, and event.

4 PROPOSED APPROACH

4.1 Overview

We now present the proposed E-CLIP framework, as shown in Fig. 2. Our goal is to unleash the potential of CLIP for event-based recognition tasks to compensate for the scarcity of large-scale event-based datasets. To this end, our E-CLIP addresses two technical challenges: 1) how to generalize CLIP’s original visual encoder to the event data while fully exploiting the event’s unique properties, *e.g.*, spatial sparsity and high temporal resolution; 2) how to effectively align the multi-modal embeddings, *i.e.*, image, text, and event, in order to achieve competitive performance in fully-supervised scenarios while preserving the exceptional few-shot capability of the CLIP model.

Consequently, we design our E-CLIP framework that consists of four major components, as depicted in Fig. 2: 1) the event encoder, responsible for extracting dense temporal and sparse spatial information from events and bridging the modality gap (Sec. 4.2.1); 2) the text encoder (Sec. 4.2.2), which incorporates content-specific information and capitalizes on pre-trained generalizing knowledge from CLIP; 3) the original CLIP’s image encoder for powerful and semantically aligned image embedding¹; 4) the hierarchical triple contrastive alignment module (Sec. 4.2.3) to jointly optimize the correlation among the three modalities embeddings generated from the three encoders, ensuring efficient information transmission among different modalities.

Overall, the already-captured and well-aligned semantics in CLIP can enhance the understanding of event data during the fine-tuning stage of the event and text encoders (Tab. 1). Furthermore, maintaining the parameters of CLIP unaltered prevents catastrophic forgetting of learned representations and preserves its few-shot ability (Tab. 2). The resulting unified feature space among the event, image, and text modalities facilitates cross-modal applications and enhances the performance of the proposed event encoder for event recognition. In the following sections, we describe these technical components.

4.2 E-CLIP Framework

4.2.1 Event Encoder

To effectively exploit the unique properties of event data, we propose a novel event encoder, based on CLIP’s image encoder. Our event encoder consists of two key technical parts: 1) event temporal modeling and 2) event prompts generation. The former performs temporal information modeling and enables temporal information exchange between event frames. The latter generates event prompts as additional modality-bridging parameters. Note that the event encoder is initialized with the CLIP image encoder’s pre-trained weights and is fine-tuned during training.

Specifically, we utilize the grid-like event frames $I_e \in \mathbb{R}^{T \times H \times W \times 3}$ with T frames of spatial size $H \times W$ as the event representation (More details can be found in the supplementary material), we divide each frame into L non-overlapping $P \times P$ square patches following the patch embedding operation of ViT [49], where $L = H \times W / P^2$. For each event frame, all patches are flattened into a $3P^2$ -dimension vector and presented as $\{x_{t,i} \in \mathbb{R}^{3P^2}\}_i^L$, where t denotes the frame number and i represents the patch number. All patch vectors are projected to D dimension by the matrix multiplication with the linear projection

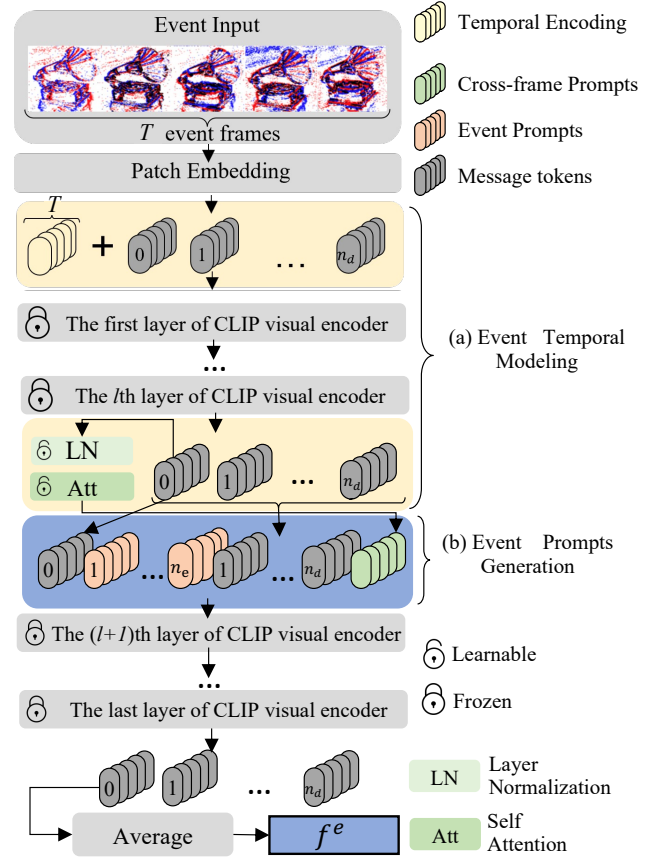


Fig. 3. **The architecture of our event encoder:** (a) event temporal modeling consisting of temporal encoding and cross-frame prompts for event spatial-temporal modeling by introducing information exchange between event frames; (b) event prompts generation, which generates event modality prompts designed to provide additional parameters for modality bridging.

$P_{emb} \in \mathbb{R}^{3P^2 \times D}$. Besides, the additional class token, namely x_{cls} , is concatenated at the beginning of the patch token sequence for each frame. The input token sequence $z_t \in \mathbb{R}^{(L+1) \times D}$ of event frame t can be formulated as:

$$z_t = LN([x_{cls}, P_{emb}^T \times x_{t,1}, P_{emb}^T \times x_{t,2}, \dots, P_{emb}^T \times x_{t,L}]), \quad (3)$$

where $LN(\cdot)$ represents the layer normalization, $[\cdot]$ means the concatenation operation; $x_{t,L}$ denotes the original message tokens, where t is the event frame number and L is the total number of patches; P_{emb} is the linear projection tensor; x_{cls} is the inserted class token.

Event Temporal Modeling. To model the unique temporal correlation among event frames, we insert temporal positional encoding into the input token sequence z_t of the event encoder as follows:

$$z_t = [x_{cls}, P_{emb}^T \times x_{t,1}, P_{emb}^T \times x_{t,2}, \dots, P_{emb}^T \times x_{t,L}] + e, \quad (4)$$

where $e = e_{spatial} + e_{temporal}$. $e_{spatial}$ and $e_{temporal}$ denote the spatial and temporal positional encoding, respectively. Following CLIP [11], $e_{spatial}$ and $e_{temporal}$ are learnable parameters and randomly initialized.

Despite the temporal positional encoding, the event encoder also presents cross-frame prompts to exchange information among event frames for better temporal information transmission. Note that, the cross-frame prompts are used in each layer of the event encoder. Concretely, for the l -th layer of the event encoder, the

1. As the image encoder in E-CLIP remains identical to CLIP, we do not elaborate on it in the following subsection.

class tokens among all T event frames are extracted from the input sequence $z_t^l, t = 1, 2, \dots, T$ and then fed into a norm layer [52] and self-attention [51] successively, aiming at obtaining the l -th layer cross frame prompts $x_{cf}^{l,t}$ as follows:

$$x_{cf}^{l,t} = \text{Att}(\text{LN}([x_{cf}^{l,1}, x_{cf}^{l,2}, \dots, x_{cf}^{l,T}])), \quad (5)$$

where $[\cdot]$ is the concatenation operation. As shown in Fig.3, the obtained cross-frame prompts, which perceive the temporal relation among frames, are concatenated with the token sequence z_t^l as input for the l -th layer in the event encoder.

Event Prompts Generation. Based on the event temporal modeling, the unique temporal correlation among event frames is captured, and the event encoder then performs event prompts generation for bridging the modality gaps among the image, text, and event. We follow the visual prompts proposed in [33], which inserts a small number of learnable parameters at the input. Consequently, the proposed event modality prompts P_e are learnable vectors inserted at the output token sequence between the original class token and the other tokens. Finally, as illustrated in Fig.3, the input token z_t^{l+1} for the $l + 1$ -th layer of the event encoder can be formulated as:

$$z_t^{l+1} = [x_{cls}, P_e^{l,t}, Z^{l,t}, x_{cf}^{l,t}], \quad (6)$$

where $P_e^{l,t}$ are the event modality prompts for the t -th frame in the l -th layer and $P_e^{l,t} = [p_1^{l,t}, p_2^{l,t}, \dots, p_{n_e}^{l,t}]$, where n_e is the number of event modality prompts; $Z^{l,t}$ is the original message token without the first class token and $Z^{l,t} = [x_1^{l,t}, x_2^{l,t}, \dots, x_{n_d}^{l,t}]$, where n_d is the number of the original message token; $x_{cf}^{l,t}$ is the cross-frame event prompts.

Through the event temporal modeling and event prompts generation, the output event embeddings of the event encoder are ultimately produced. Specifically, for an event encoder E_e with S layers, it obtains the event embedding z_t^l of frame t at layer l as follows:

$$z_t^l = E_e^l(z_t^{l-1}), l \in 1, 2, \dots, S. \quad (7)$$

Subsequently, the class token $f^{e,t} \in \mathbb{R}^{D'}$, which represents the event class prediction, is extracted from the first token of the last layer token sequence z_t^S for each event frame t , and then projected to the D' dimension using the linear projection $P_{cls} \in \mathbb{R}^{D \times D'}$. To exchange temporal information among event frames and obtain the final prediction, as shown in Fig.3, we average the event class token $f^{e,t}$ among all event frames and obtain the final event embedding f^e .

4.2.2 Text Encoder

Having introduced the novel event encoder that addresses the challenge of generalizing CLIP’s original visual encoder to event data, we subsequently propose a novel text encoder to better align text with events. Specifically, the text encoder generates content prompts to enhance fine-tuning performance and incorporates hybrid text prompts—combining hand-crafted and learnable prompts—to improve generalization across diverse datasets. Additionally, a loss function is introduced to enforce semantic consistency between the text embeddings generated from the hand-crafted and learnable prompts.

Content Prompts Generation is first introduced to augment the text encoder by incorporating additional content prompts, thereby

enhancing recognition performance. In the CLIP model, the hand-crafted text prompts ‘A photo of a $[cls]$ ’ are utilized as input for the text encoder, where $[cls]$ represents the category name. This text prompt is then transformed into text tokens $P_h^t \in \mathbb{R}^{5 \times D_p}$ using CLIP’s tokenizer, wherein each word is converted into a D_p -dimensional word embedding.

The content prompts are generated by a simple and lightweight MLP, which takes the event embeddings f^e and image embeddings f^i as input and produces the corresponding event content prompts $\sigma_e \in \mathbb{R}^{1 \times D_p}$ and the image content prompts $\sigma_i \in \mathbb{R}^{1 \times D_p}$. The obtained content prompts σ_e and σ_i have the same dimension D_p as the hand-crafted text token P_h^t so as to be added with it. The MLP is a bottleneck structure with two linear layers and one activation function, thereby avoiding excessive computational overhead while achieving effective results.

Hybrid Text Prompts Empirically, we find that the model’s fine-tuned performance and zero-shot ability are contradictory. That is, the higher the fine-tuned performance, the lower the zero-shot score the model can achieve. This arises from the overfitting of ‘seen’ classes among small datasets compared to CLIP’s four million image-text training pairs with numerous variations. A similar phenomenon is observed in CoOp [25], where learnable text prompts obtain enhanced fine-tuned performance but a substantial drop in zero-shot ability (69.34% (CoOp) vs 82.89% (CLIP)).

To address this dilemma, KgCoOp [27] introduces both learnable and hand-crafted text prompts to reduce the discrepancy between them using the MSE loss function. Motivated by this, we propose the hybrid text prompts, which comprise hand-crafted text prompts and learnable text prompts to enhance the generalization ability of our E-CLIP. Specifically, the learnable text prompts can be formulated as $P_l^t = [p_1^t, p_2^t, \dots, p_{n_l}^t, cls, \cdot]$, where $p_i, i = 1, 2, \dots, n_l$, is a vector with the same dimension as the hand-crafted text token P_h^t ; n_l denotes the number of the learnable text prompts; cls represents the tokenized word embeddings and $[\cdot]$ means the concatenation operation.

Next, the learnable text prompts P_l^t and the hand-crafted text prompts P_h^t are added with the content prompts σ_m , respectively, generating the final text input, as depicted in Fig.2. This text input is then fed into the text encoder to obtain improved fine-tuned performance and few-shot ability. Finally, the text embeddings $f_l^{t,m}$ and $f_h^{t,m}$ generated from the learnable and hand-crafted prompts are produced by the text encoder E_t :

$$f_l^{t,m}, f_h^{t,m} = E_t(P_{l,m}^\sigma), E_t(P_{h,m}^\sigma). \quad (8)$$

where the MSE loss is employed to reduce the gap between $f_l^{t,m}$ and $f_h^{t,m}$. The final text embedding $f^{t,m}, m = e, i$ of modality m is obtained by averaging the $f_l^{t,m}$ and $f_h^{t,m}$.

Overall, we can obtain the image, event, and text embeddings from the original image encoder, the proposed event encoder, and text encoders, respectively. In the following section, we describe how to align the triple modality embeddings with the proposed Hierarchical Triple Contrastive Alignment (HTCA) module.

4.2.3 Hierarchical Triple Contrastive Alignment (HTCA)

In the task of event recognition, a simple pretraining objective involves aligning the event embedding feature f^e and the text embedding feature f^t into a unified representation space from scratch. However, due to the relatively small size of the event dataset, it is not guaranteed that both the event and text encoders can generate reliable representations. Moreover, the limited

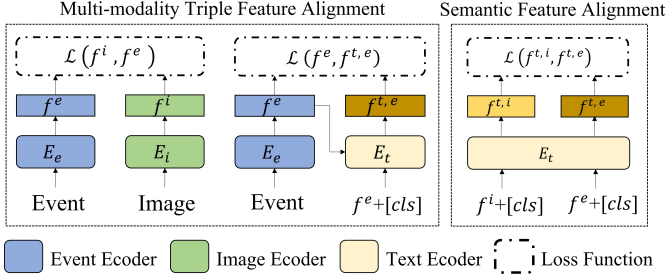


Fig. 4. Overview of total objective. The details are elaborated in Sec.4.3.

learned text vocabulary space, when compared to the vast number of real-world items, can lead to poor zero-shot performance.

To address these challenges, we propose a Hierarchical Triple Contrastive Alignment (HTCA) module based on the image-text pre-trained feature space of CLIP [11]. This module aims to optimize the correlation alignment among event, image, and text jointly. The proposed HTCA module consists of two components: *multi-modality triple feature alignment* and *semantic feature alignment*, as illustrated in Fig. 2.

Multi-modality Triple Feature Alignment To jointly align the triple modalities, we first minimize the contrastive loss between the event embedding and both the image and text embeddings, forming event-image and event-text pairs. Note that we disregard the image-text pair during the experiment because we empirically observe that any attempt to alter the pre-trained image-text alignment results in a performance drop.

Specifically, as shown in Fig. 2, the input image is encoded by the CLIP’s frozen image encoder, generating the visual embedding $f^i \in \mathbb{R}^{1 \times D}$, where D denotes the embedding dimension. Meanwhile, the event embeddings $f^e \in \mathbb{R}^{1 \times D}$ are extracted by the proposed event encoder (Sec. 4.2.1). Then, the text encoder generates content prompts from the event features f^e (Sec. 4.2.2) and obtains the final event content added text embedding $f^{t,e} \in \mathbb{R}^{1 \times D}$.

The contrastive loss for the n -th sample within a mini-batch among each pair of modalities M_1 and M_2 is computed as follows:

$$l(n, M^1, M^2) = -\log \frac{\exp(M_n^1 \cdot M_n^2 / \tau)}{\exp(M_n^1 \cdot M_n^2 / \tau) + \sum_{m \in N, m \neq n} \exp(M_n^1 \cdot M_m^2 / \tau)}, \quad (9)$$

where τ is the temperature coefficient, N represents the size of the mini-batch, n, m denote the n -th and the m -th data of the mini-batch, $m \neq n$, and $m = n$ indicates the negative pair and positive pair in a training batch respectively. Then the contrastive loss value is averaged among the whole mini-batch. The final $L(M^1, M^2)$ can be described as:

$$L(M^1, M^2) = \frac{1}{N} \sum_{n \in N} l(n, M^1, M^2) \quad (10)$$

Lastly, we introduce the contrastive loss $L_{i\&e}(f^i, f^e)$ between event and visual embedding f^e and f^i . When it comes to the event-text pair, we utilize the contrastive loss $L_{t\&e}(f^e, f^{t,e})$ to align the event embedding f^e and the event content added text embedding $f^{t,e}$.

Semantic Feature Alignment Despite the multi-modality triple feature alignment, the embeddings from three modalities are

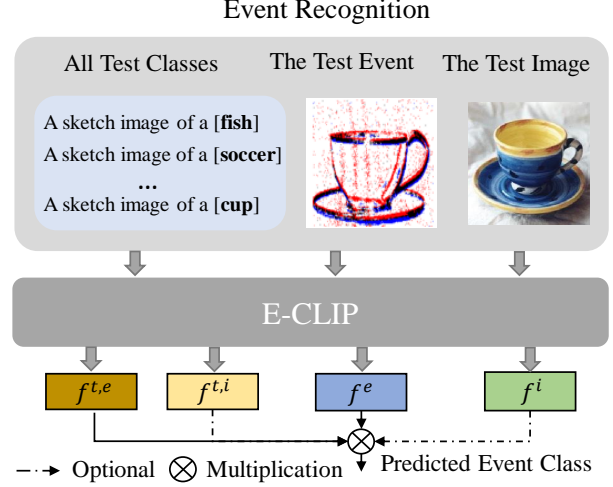


Fig. 5. The configuration of our E-CLIP for the recognition task.

aligned, we also introduce semantic feature alignment between the text embeddings generated from the image and event content to inherit the remarkable zero-shot ability of the pre-trained CLIP. Specifically, we ensure the semantic consistency between the final text embedding $f^{t,i} \in \mathbb{R}^{1 \times D}$ and $f^{t,e} \in \mathbb{R}^{1 \times D}$ from image and event input data, with contrastive loss function $L_t(f^{t,i}, f^{t,e})$.

4.3 Total Objective

In summary, as shown in Fig. 4.3, the final loss function is composed of $L_{i\&e}(f^i, f^e)$, $L_{t\&e}(f^e, f^{t,e})$ and $L_t(f^{t,i}, f^{t,e})$ from Sec. 4.2.3, as well as the MSE loss mentioned in Sec. 4.2.2. We combine them with different trade-off hyper-parameters,

$$L_{final} = \alpha \times L_{i\&e}(f^i, f^e) + \beta \times L_{t\&e}(f^e, f^{t,e}) + \theta \times L_t(f^{t,i}, f^{t,e}) + \gamma \text{MSE}(f_l^{t,m}, f_h^{t,m}), \quad (11)$$

where $f^e, f^i, f^{t,e}, f^{t,i}$ denotes the event embeddings, image embeddings, event content added text embeddings and image content added text embeddings; $\text{MSE}(\cdot)$ indicates the mean squared error loss function; $f_l^{t,m}$ and $f_h^{t,m}$ is the text embedding generated from the learnable and hand-crafted text prompts for modality m , respectively, where m can be e for event modality or i for image modality. Note that we set the default values of α, β, θ , and γ to 1 since the frozen CLIP visual encoder serves as the initialization of the event encoder, ensuring that the magnitudes of the three losses are distributed on the same scale.

5 EXPERIMENTS

5.1 Using E-CLIP

Event Recognition It is the process of classifying event data, which is a fundamental task in event-based vision. A model with exceptional event feature extraction capability can achieve superior recognition performance, serving as the foundation for more complex tasks such as event tracking, detection, segmentation, and scene understanding. As shown in Fig. 5, all text class names are input into the text encoder, generating event content prompts-added text embedding $f^{t,e}$ for all classes. The event encoder subsequently encodes the test event data to produce the event embedding f^e , and optionally, the image embedding of the test image. The softmax function is applied to the multiplication of

TABLE 1
Fine-tuned performance. ‘-’ represents the exact number not provided.

Method	Pretrain Dataset	Labels	Top1 Accuracy		
			N-Caltech101	N-MNIST	N-ImageNet
<i>Transfer learning of event self-supervised pre-training methods.</i>					
HATS [43]	✗	✗	64.20	99.10	47.14
AEGNN [53]	✗	✗	66.80	-	-
AsynNet [54]	✗	✗	74.50	-	-
EvS-S [8]	✗	✗	76.10	-	-
<i>Transfer learning of image supervised pre-training methods.</i>					
RG-CNN [55]	✗	✓	65.70	99.00	-
EST [3]	ImNet-1k	✓	81.70	-	48.93
DVS-ViT [56]	ImNet-21k	✓	83.00	-	-
Matrix-LSTM [57]	✗	✓	84.31	98.90	32.21
E2VID [58]	ImNet-1k	✓	86.60	98.30	-
DiST [4]	✗	✓	86.81	-	48.43
EventDrop [59]	ImNet-1k	✓	87.14	-	-
ACE-BET [9]	ImNet-1k	✓	89.95	-	-
<i>Transfer learning of image-text supervised pre-training methods.</i>					
ELIP(Our Model)	WIT	✓	93.89	99.20	51.85

TABLE 2

Zero-shot & Few-shot performance compared with the EventCLIP. ‘-’ represents the exact number not provided; ‘Δ’ refers to the improvement.

Setting	E-CLIP (Our method)			EventCLIP [10]	
	N-Caltech101	N-Imagenet	N-MNIST	N-Caltech101	N-Imagenet
0-shot	50.40	4.31	18.77	70.76	21.37
1-shot	66.72	22.22	64.32	75.42	24.30
2-shot	75.87	26.85	77.46	80.53	25.74
5-shot	82.35	28.70	85.34	81.53	26.85
10-shot	86.92	30.56	90.83	83.52	28.60
20-shot	90.51	35.11	95.43	85.89	30.48

all embeddings, resulting in the final probability map, where the highest score indicates the predicted category. Depending on the size of event data used during training, event recognition can be classified into three groups.

Fine-tuning Event Recognition makes use of the entire training dataset so that the model achieves enhanced performance when recognizing the limited classes present in the training dataset. Fine-tuning pre-trained models is an effective strategy for improving the performance of downstream tasks or a new dataset. Because of its well-aligned event-image-text feature space, Our proposed E-CLIP framework can serve as a valuable starting point for fine-tuning.

Few-shot Event Recognition is defined by the number of training examples for a single category used during the training procedure. In reality, real-world event data and their corresponding labels are relatively rare and valuable, compared with the abundance of currently available large-scale image datasets. Owing to the powerful transferability enabled by the pre-trained representation space, our E-CLIP model also supports few-shot event recognition.

To evaluate the effectiveness of our E-CLIP, we conduct extensive experiments on two event-based tasks, including event recognition and event retrieval sample, implementing zero-shot, few-shot, and finetune settings for comprehensive model evaluation. The subsequent subsections describe the experiments’ configuration, results, and analyses in detail.

5.2 Experimental Setup

Dataset We select three publicly available image-event-text paired datasets for the experiments, including N-ImageNet [4] paired with ImageNet-1K [60], N-Caltech101 [61] paired with Caltech101 [62] and N-MNIST [62] paired with MNIST [63], whose

event recognition difficulty declines as the number of dataset’s categories decrease.

N-ImageNet [4] dataset is derived from the ImageNet-1K dataset, in which the RGB images are displayed on a monitor and captured with a moving event camera. It has a similar structure to the ImageNet-1K dataset and contains 1,781,167 event data samples covering 1,000 distinct object classes. All event data in this dataset have 480×640 resolution. **N-Caltech101** [61] and **N-MNIST** [62] datasets are relatively small datasets. N-Caltech101 is composed of event streams captured using an event camera in front of a moving 180×240 resolution ATIS system [64] in front of the LCD monitor presenting the original RGB images in Caltech101. There are 8,246 samples comprising 300 ms in length, covering 101 different types of items. Similarly, N-MNIST is created by displaying a moving image from the MNIST dataset on the LCD monitor and recorded with the ATIS system. It’s a containing 70,000 event data samples covering 10 hand-written numbers 0 to 9.

During pre-training, we utilize the official partitions of the training and validation datasets for N-ImageNet and N-MNIST datasets. The N-Caltech101 dataset is randomly divided into training and validation datasets in a 4:1 ratio. For the zero-shot, few-shot, and fine-tuning evaluation, we consistently utilize the same validation set.

Dataset Preprocessing We resize all images from the above-mentioned different datasets to a resolution of 224×224 to maintain consistency with the ViT input settings. Also, we convert each grayscale image in the dataset to a three-channel tensor by concatenating three identical copies.

When preprocessing the event stream, we normalize its length by either padding short event data with 0 or removing excess

TABLE 3
Ablation study on different combinations of the proposed modules.

HTCA	Ablation		Top1 Accuracy			
	Prompts in the text encoder	Event encoder	N-Caltech101	Δ	N-MNIST	Δ
\times	\times	\times	50.40	-	18.77	-
\checkmark	\times	\times	92.54	+42.14	96.49	+77.72
\checkmark	\checkmark	\times	93.40	+43.00	98.95	+80.18
\checkmark	\checkmark	\checkmark	93.87	+43.47	99.20	+80.43

TABLE 4
Ablation study on the Triple alignment loss function

$L(f^e, f^i)$	Ablation Setting		Top1 Accuracy			
	$L(f^e, f^{t,e})$	$L(f^{t,i}, f^{t,e})$	N-Caltech101	Δ	N-MNIST	Δ
\times	\times	\times	50.40	-	18.77	-
\checkmark	\times	\times	70.31	+19.91	57.95	+39.18
\times	\checkmark	\times	90.35	+39.95	97.61	+78.84
\checkmark	\checkmark	\times	92.47	+42.07	98.51	+79.74
\checkmark	\checkmark	\checkmark	93.33	+42.93	98.83	+80.06

event data for longer sequences. We aggregate every fixed number of continuous event data to create event frames, where the event stream’s length is set to 40000, 20000, and 10000 for N-ImageNet, N-Caltech101, and N-MNIST datasets, yielding 5, 5, and 3 event frames in total respectively. We determine these values based on the event data resolutions for each dataset and the visualization effect of stacked frame-like event images.

For the RGB event frame-like representation, we colorize the positive and negative event counts by multiplying them with [0, 255, 255] and [255, 255, 0], respectively. To normalize the data within the range of 0 to 255, we apply the clip function. On the other hand, for the ‘Gray-scale’ mode, we colorize both positive and negative event counts from the 2-channel event histograms by multiplying them with [127, 127, 127]. The resulting colored event counts are then added together to generate the final three-channel images.

Experimental Settings For the pre-trained CLIP, we employ the ViT-B/16 [65] image encoder and the Transformer-based text encoder [51]. The event encoder is initialized from CLIP image encoder pre-trained weights. We utilize “A sketch image of a [cls]” as the hand-crafted text prompts template. The Pytorch [66] framework serves as the foundation for all experiments. The Adam [67] optimizer is adopted to train our network. The initial learning rates are set to 1e-5 for N-Caltech and N-MNIST datasets and 1e-6 for N-Imagenet. The weight decay is 2e-4. CosineAnnealingLR [68] learning rate schedule is utilized and the minimal learning rate is 1e-8. We use the Adam optimizer over 8 RTX 3090 GPUs with a total of 64 images-event-text pairs per mini-batch. All few-shot experiments are trained for 30 epochs. For finetuning experiments, our model is trained for 30 epochs for N-Caltech. Due to the relatively small object number of the N-MNIST dataset, we decrease the epoch number to 15 to prevent overfitting. Moreover, due to the computational cost, we only finetuning E-CLIP on N-Imagenet for 3 epochs. However, additional training epochs and hyperparameter searching, we believe, could boost performance further. Our code and pre-trained models will be publicly available.

5.3 Event recognition results

5.3.1 Fine-tuning Experiments

We present the results of our fine-tuning experiments in Tab. 1 on N-Caltech101, N-MINIST, and N-ImageNet datasets. We compare

our proposed E-CLIP with various baselines, including event self-supervised pre-training methods [8], [43], [53], [54], [69], [70] and transfer learning of supervised image pretraining methods [3], [9], [56], [58], [59]. E-CLIP utilizes the weights of CLIP pre-trained on a web-scale image-text dataset (WIT) and transfers them to the event modality with a small number of fine-tuning epochs, making it computationally efficient yet effective. *our E-CLIP achieves new state-of-art accuracy compared with the previous method on three benchmarks.* For the **N-Caltech101 dataset**, our fine-tuning model achieved a top-1 accuracy of **93.89%**, surpassing the previous state-of-the-art accuracy by **+3.94%**. In a similar vein, with a mere three epochs of fine-tuning on the **N-ImageNet dataset**, E-CLIP attains an accuracy of **51.85%**, exhibiting a notable increase of **2.92%** when compared to prior methodologies. We believe extra training epochs and extensive hyperparameter searching might potentially enhance performance to a greater extent. For **N-MNIST dataset**, E-CLIP also achieves a new state-of-the-art accuracy of **99.20%**, compared to the previous 99.10% achieved by the HATS [43]. Although our E-CLIP does not significantly outperform the existing method, this is attributed to the existing high accuracy (99.1%) and the limitations of the relatively small object number (ten classes) in the N-MNIST dataset. The above fine-tuning results clearly demonstrate E-CLIP’s powerful embedding space where event data is effectively aligned with semantic meaning. In addition, achieving competitive performance on datasets containing 10, 101, and 1,000 distinct object classes without overfitting demonstrates the adaptability of our proposed framework.

5.3.2 Zero-shot and Few-shot Experiments

Tab. 2 illustrates the results of zero-shot and few-shot experiments performed on test sets of the N-Caltech101, N-MINIST, and N-ImageNet datasets. We compare the performance of our proposed E-CLIP with the closely related work, EventCLIP [10], specifically on the N-Caltech101 and N-ImageNet datasets. Notably, our E-CLIP outperforms it in few-shot scenarios, achieving a significant improvement of **3.91%** and **4.92%** for 10-shot and 20-shot settings on the N-Caltech101 dataset. *Note that our 20-shot accuracy (90.51%) even surpasses the previous best classifier trained on the entire dataset (89.95% achieved by the ACE-BET [9]) with the usage of only 46.09% data of the N-Caltech101 dataset.* For the N-ImageNet dataset, our E-CLIP also surpasses

TABLE 5
Ablation study on event prompts generation module

Setting		Top1 Accuracy				
Event Modality	Prompts	Cross-frame Prompts	N-Caltech101	Δ	N-MNIST	Δ
\times		\times	68.98	-	59.95	-
\times		\checkmark	71.07	+2.09	61.24	+1.29
\checkmark		\times	71.24	+2.26	63.02	+3.07
\checkmark		\checkmark	72.51	+3.53	65.02	+5.07

its competitor with **1.96%** and **4.63%** improvement for 10-shot and 20-shot settings. The above few-shot results demonstrate the superiority and label efficiency of our E-CLIP model in the low-shot regime.

In the zero-shot settings, our E-CLIP falls short of surpassing the performance of the previous method EventCLIP, mainly because EventCLIP uses the ‘gray-scale’ event frame directly as input to the CLIP visual encoder without introducing additional parameters. However, in E-CLIP, the event encoder and the hybrid text prompt in the text encoder introduce extra parameters, affecting the zero-shot performance. Additionally, E-CLIP achieves only 18.77% for zero-shot performance on the N-MNIST dataset. This can be explained by the suboptimal image recognition performance of the original CLIP on the MNIST dataset, where the linear probe results of zero-shot CLIP are 10% worse than the ResNet50 result for the MNIST dataset [11]. Nevertheless, E-CLIP demonstrates outstanding transferability to unknown event datasets, attaining a remarkable 96.43% performance for event recognition on the N-MNIST dataset in the 20-shot setting.

6 ABLATION STUDY

Effectiveness of the proposed HTCA, event encoder, and text encoder We conduct ablation experiments on the N-Caltech101 and N-MNIST datasets to evaluate the effectiveness of our proposed HTCA module, hybrid text prompts in the text encoder, and event encoder. The detailed results with different combinations are presented in Tab. 3. Notably, all of them positively impact the fine-tuning recognition accuracy. Specifically, the HTCA shows significant performance gains of **+42.14%** and **+77.72%** on the two benchmarks, respectively. Furthermore, based on the proposed HTCA, the text prompts in the text encoder provide additional improvements of **+43.00%** and **+80.18%** accuracy on the respective datasets. Lastly, when combining all of them, the accuracy increases from 50.40% and 18.77% to 93.87% and 99.20%, representing substantial **+43.47%** and **+80.43%** performance gains. *These results demonstrate the effectiveness of our proposed modules in significantly improving the overall performance of the model.*

The effectiveness of HTCA module We study the effectiveness of the HTCA module on both the N-Caltech101 and N-MNIST datasets. As shown in Tab. 4, the contrastive loss $L(f^e, f^i)$ between the event and image embeddings improves the zero-shot baseline accuracy by **+19.91%** and **39.18%** on the N-Caltech101 and N-MNIST datasets, respectively. The contrastive loss $L(f^e, f^{t,e})$ between the event embedding f^e and the event content added text embedding $f^{t,e}$ contribute positively to the accuracy with increases of **+39.95%** and **78.84%**. We also investigate the combination of $L(f^e, f^i)$ and $L(f^e, f^{t,e})$ in our E-CLIP framework, which results in a substantial accuracy gain of **+42.07%** and **+79.74%** on the two datasets. Furthermore,

TABLE 6
Ablation study on training configuration.

Setting	Top1 Accuracy	
	N-Caltech101	N-MNIST
Frozen CLIP	86.69	97.11
Fitune CLIP	93.29	98.51

TABLE 7
Ablation study on event representation.

Setting	Top1 Accuracy	
	N-Caltech101	N-MNIST
Gray-scale frame-like	92.18	97.61
RGB frame-like	92.50	98.23

when both multi-modality triple feature alignment and the semantic feature alignment were combined, they improve the zero-shot baseline accuracy by **+43.93%** and **+80.06%**. *These results demonstrate the effectiveness of the HTCA module in enhancing the performance of our E-CLIP framework.*

The ablation study on event encoder To validate the effectiveness of our proposed event encoder, we conducted experiments on two benchmarks employing various event prompt combinations. As illustrated in Table 5, event modality prompts positively impact recognition accuracy, yielding improvements of **+2.09%** and **+1.29%** on the N-Caltech101 and N-MNIST datasets, respectively. Furthermore, cross-frame prompts also contribute positively to recognition accuracy, exhibiting increases of **+2.26%** and **+3.07%**. Notably, when utilizing both prompts concurrently, we attain even higher recognition accuracy, with enhancements of **+3.53%** and **+5.07%** on both datasets. *These outcomes corroborate the effectiveness of our proposed event prompt generation module, which furnishes supplementary modality-bridging parameters, as asserted in Section 1.*

Fine-tune CLIP vs. Frozen CLIP as the event encoder backbone The Event Encoder in E-CLIP derived from the original CLIP image encoder is a crucial component for harnessing the event’s unique properties. The ablation results are shown in Tab. 6, where we ablate to freeze and fine-tune the CLIP image encoder as the Event Encoder. As we can see, using the frozen CLIP image encoder as the event feature extractor only achieves 86.69% and 97.11% recognition accuracy. *Obviously, fine-tuning the CLIP image encoder as the Event Encoder improves the accuracy to 93.29% and 98.51%.*

Event representation Tab. 7 presents the ablation of different methods of colorizing the frame-like event representations. Using the gray-scale frame-like event representation achieves 92.19% and 97.61% recognition accuracy while using RGB frame-like event representation improves the accuracy to 92.50% and 98.23% respectively. *The RGB frame-like event representation performs better because it closely resembles the natural images that CLIP*

TABLE 8
Ablation study on the content prompts generation module.

Ablation settings		Top1 Accuracy			
Image content prompts	Event content prompts	N-Caltech101	Δ	N-MNIST	Δ
\times	\times	91.96	-	98.51	-
\times	\checkmark	92.25	+0.29	98.67	+0.16
\checkmark	\times	92.82	+0.86	98.72	+0.21
\checkmark	\checkmark	93.00	+1.04	98.86	+0.35

is pre-trained on.

The length of event modality prompts We investigate how the length of the event modality prompts impacts the effectiveness of event recognition. We test different lengths of event modality prompts, *i.e.*, 4, 8, and 16. As shown in Fig. 7 (b), using 16 as the length of the event modality prompts achieves the best recognition accuracy of **92.92%** and **98.71%** on the N-Caltech101 and N-MNIST dataset respectively. Even though the accuracy shows an upward trend with the increasing length of event modality prompts, we don’t evaluate longer event modality prompts because introducing longer event modality prompts yields diminishing returns but exponentially increases the computational cost.

Effectiveness of the content prompts generation In E-CLIP, we introduce the content prompt generation in the text encoder to enhance the text encoder prompts by incorporating additional content prompts, specifically the image content and the event content. To individually investigate the effectiveness of image and event content prompts, we provide the results with different content prompts combinations in Tab. 8. Using the image content prompts alone brings a **+0.29%** and **+0.16%** accuracy improvement compared to the baseline without any content prompt, while using the event content prompts alone results in a **+0.86%** and **+0.21%** accuracy improvements on N-Caltech101 and N-MNIST datasets. Combining these two modalities of content prompts achieves a higher accuracy gain of **+1.04%** and **+0.35%** on both datasets. *These results demonstrate the effectiveness of our proposed content prompt generation in enhancing the performance of the E-CLIP framework.*

The effectiveness of hybrid text prompts We conduct the ablation study on the hybrid text prompts to evaluate its impact on fine-tuning performance and generalization ability. The experiment follows the setting proposed in [25], where the entire dataset is divided into the base and new datasets, each containing half of the object classes. For each ablation setting, the model is fine-tuned on the base set without being exposed to half of the event classes in the new set. The evaluation is then performed on the new set to assess the generalization ability. As shown in Tab. 9, the utilization of the hand-crafted text prompts achieves an impressive 72.55% top-1 accuracy on the new set for the N-Caltech dataset, showcasing its remarkable zero-shot ability. Conversely, the learnable text prompts enhance the fine-tuning performance on the base set, but this comes at the cost of reduced accuracy on the new set due to its limited generalization ability. *In contrast, our proposed hybrid text prompts module, which combines both learnable and hand-crafted text prompts, achieves the highest fine-tuning accuracy of 91.23% with a smaller decline in zero-shot performance compared to using single hand-crafted text prompts. (-10.70% V.S -4.53% for N-Caltech101).* For N-MNIST dataset, it is unsurprising that the model achieves very low accuracy on the base dataset when using hand-crafted text prompts, which maintains the same accuracy as the zero-shot results shown in Tab. 2. This is due to the poor

image recognition performance of the original CLIP on the N-MNIST dataset (zero-shot CLIP results are 10% worse than the linear probe on ResNet50 for the MNIST dataset [11]). *Our model with the hybrid text prompts module achieves top-one accuracy on both the base dataset(93.56%) and the new dataset(98.86%) for the N-MNIST dataset, demonstrating the effectiveness of our proposed module.*

The initialization of hand-crafted text prompts We design four kinds of hand-crafted text prompts to find out which generated text embeddings can be better aligned with the event embeddings. The results of the experiments are shown in Tab. 10, and the hand-crafted text prompts "A sketch image of [cls]" achieves the best results of **93.21%** and **99.04%** on N-Caltech101 and N-MNIST datasets. *The experimental results show that since event data mainly capture boundary information, prompts like "sketch image" can bring better performance [10] and help the text better align with event representations.*

The length of text learnable prompts We also examine the influence of the length of the learnable text prompts on the effectiveness of event object recognition. We test various lengths of learnable text prompts, *i.e.*, 4, 8, and 16. *As demonstrated in Fig.7 (b), employing 16 as the length of the event modality prompts achieves the best recognition accuracy.* Although the accuracy exhibits an upward trend with the increasing length of event modality prompts, we do not evaluate longer learnable text prompts for the same reason in Sec. 6.

7 EXTENSION EXPERIMENTS

Beyond the event recognition task, we show that our method can be flexibly extended to the image-to-event and text-to-event retrieval tasks.

7.1 Event Retrieval

The process of searching for event stream data that is similar to a given query, which might be of any modality, such as an image or text, is known as event retrieval. This has a wide range of practical uses, such as matching a real-world object with its associated event data based on a single image or text description. To retrieve data using our proposed E-CLIP, as shown in Fig. 8, we utilize the pre-trained event encoders to generate all test event embeddings f^e . Using the identical method, we obtain the query image and text embeddings using their corresponding encoders. Following that, we multiply the similarity score between the query embeddings and event embeddings and retrieve the event data with the highest similarity scores. We follow an identical procedure for the zero-shot, few-shot, and fine-tuning experiments for event retrieval the way we carry out the event recognition experiments, so we do not elucidate further.

TABLE 9
Ablation study on hybrid text prompts module.

Ablation settings		Base		New	
Learnable	Hand-crafted	N-Caltech101	N-MNIST	N-Caltech101	N-MNIST
✗	✓	90.57	91.03	72.55	18.80
✓	✗	91.01	93.22	61.85	46.02
✓	✓	91.23	93.56	68.02	49.92

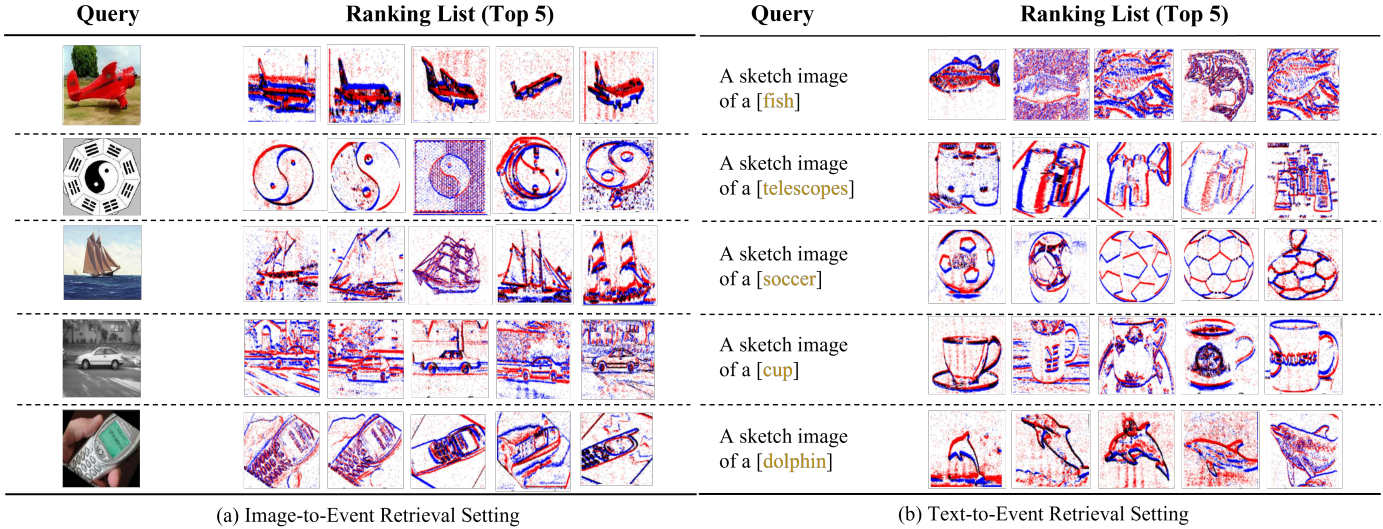


Fig. 6. Retrieving event data from an event-image paired database (N-Caltech101) using random image and text queries, where event data are visualized in frame-based representation.

TABLE 10
Ablation study on the hand-crafted text prompts.

Hand-crafted text prompts	Top1 Accuracy	
	N-Caltech101	N-MNIST
A photo of a	93.06	98.53
A sketch image of a	93.21	99.04
A point cloud image of a	92.71	98.49
An event frame of a	92.41	98.87

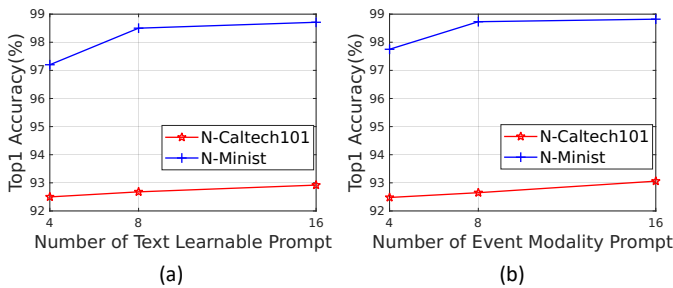


Fig. 7. Ablation studies on (a) the number of text learnable prompts and (b) the number of event modality prompts.

7.2 Event Retrieval Results

In this paper, we make the **first** attempt at conducting the event retrieval task employing both text and image queries. To evaluate the event retrieval performance, we utilize the indexes Recall@1, Recall@5, and Recall@10, widely utilized in retrieval tasks [71], [72]. The experimental results in Fig. 9 demonstrate the effectiveness of our E-CLIP across different experimental settings, including zero-shot, few-shot, and fine-tuning settings. Evidently,

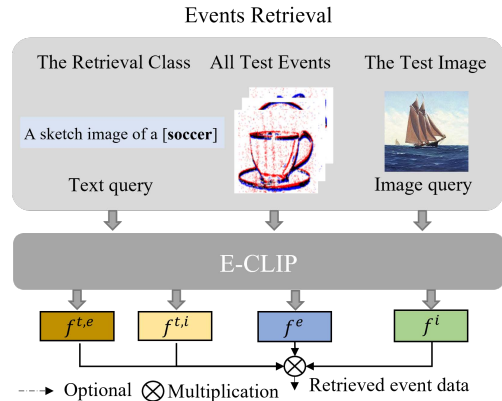


Fig. 8. Extension experiment: E-CLIP for event data retrieval.

our E-CLIP shows remarkable retrieval performance (**99.01% Recall@1** for text query and **96.70% Recall@1** for image query) with only 20 shot training examples, demonstrating its remarkable capabilities in few-shot learning. Notably, in both text-to-event retrieval and image-to-event retrieval settings, our model achieves an impressive recall rate, reaching close to **100.00% on Recall@1** after fine-tuning. *This exceptional performance indicates that our model effectively aligns event embeddings with the embeddings of both images and text.*

For visualization, we randomly select images from the Caltech101 dataset as the image queries, and N-Caltech101 functions as our event library for retrieval. We display in Fig. 6 five event data with the maximum similarity to the image query. Similarly, we utilize random text queries and exhibit the best matches. All

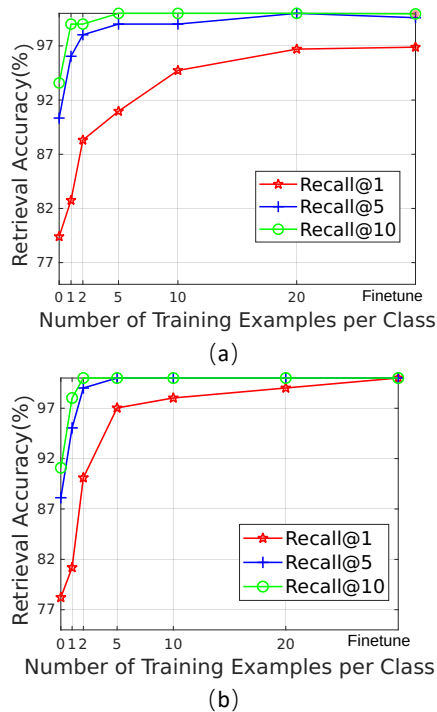


Fig. 9. Event Retrieval results on N-Caltech101 dataset with zero-shot, few-shot, and fine-tuning settings. (a) Image-to-event retrieval. (b) Text-to-event retrieval.

the retrieved event data have a very high degree of similarity to the input text query, demonstrating the effectiveness of our proposed E-CLIP framework.

8 CONCLUSION

In this paper, we addressed the challenging tasks of generalizing the CLIP model to event data while aligning the multi-modal embeddings among images, text, and events. To this end, we proposed E-CLIP, a novel framework that capitalizes on the potential of CLIP for event-based recognition tasks to compensate for the lack of large-scale event-based datasets. We introduced novel event and text encoders designed to exploit the unique properties of event data and enhance its generalization ability. Furthermore, we proposed a hierarchical triple contrastive alignment to optimize the correlation alignment among these three distinct modalities. Extensive experiments on three object recognition benchmarks demonstrated the superiority and label efficiency of our proposed E-CLIP. Extension experiments on event retrieval indicated that our E-CLIP possesses excellent generalization ability. In the future, we plan to extend our method to handle more high-level event-based tasks. Meanwhile, we hope that our E-CLIP will facilitate the incorporation of knowledge from the text modality into the event-based vision, thereby harnessing decades of valuable research and contributing to the development of a more principled framework.

REFERENCES

- [1] X. Zheng, Y. Liu, Y. Lu, T. Hua, T. Pan, W. Zhang, D. Tao, and L. Wang, "Deep learning for event-based vision: A comprehensive survey and benchmarks," *arXiv preprint arXiv:2302.08890*, 2023.
- [2] G. Gallego, T. Delbrück, G. Orchard, C. Bartolozzi, B. Taba, A. Censi, S. Leutenegger, A. J. Davison, J. Conradt, K. Daniilidis *et al.*, "Event-based vision: A survey," *IEEE transactions on pattern analysis and machine intelligence*, vol. 44, no. 1, pp. 154–180, 2020.
- [3] D. Gehrig, A. Loquercio, K. G. Derpanis, and D. Scaramuzza, "End-to-end learning of representations for asynchronous event-based data," in *Proceedings of the IEEE/CVF International Conference on Computer Vision*, 2019, pp. 5633–5643.
- [4] J. Kim, J. Bae, G. Park, D. Zhang, and Y. M. Kim, "N-imagenet: Towards robust, fine-grained object recognition with event cameras," in *Proceedings of the IEEE/CVF international conference on computer vision*, 2021, pp. 2146–2156.
- [5] Y. Wang, B. Du, Y. Shen, K. Wu, G. Zhao, J. Sun, and H. Wen, "EV-Gait: Event-based robust gait recognition using dynamic vision sensors," in *CVPR*, 2019.
- [6] X. Lagorce, F. Orchard, Garrick and Galluppi, B. E. Shi, and R. B. Benosman, "Hots: a hierarchy of event-based time-surfaces for pattern recognition," *TPAMI*, 2016.
- [7] F. Gu, W. Sng, T. Taunyazov, and H. Soh, "Tactilesnet: A spiking graph neural network for event-based tactile object recognition," in *IROS*, 2020.
- [8] Y. Li, H. Zhou, B. Yang, Y. Zhang, Z. Cui, H. Bao, and G. Zhang, "Graph-based asynchronous event processing for rapid object recognition," in *Proceedings of the IEEE/CVF International Conference on Computer Vision*, 2021, pp. 934–943.
- [9] C. Liu, X. Qi, E. Y. Lam, and N. Wong, "Fast classification and action recognition with event-based imaging," *IEEE Access*, vol. 10, pp. 55 638–55 649, 2022.
- [10] Z. Wu, X. Liu, and I. Gilitschenski, "Eventclip: Adapting clip for event-based object recognition," *arXiv preprint arXiv:2306.06354*, 2023.
- [11] A. Radford, J. W. Kim, C. Hallacy, A. Ramesh, G. Goh, S. Agarwal, G. Sastry, A. Askell, P. Mishkin, J. Clark *et al.*, "Learning transferable visual models from natural language supervision," in *International conference on machine learning*. PMLR, 2021, pp. 8748–8763.
- [12] S. T. Wasim, M. Naseer, S. Khan, F. S. Khan, and M. Shah, "Vita-clip: Video and text adaptive clip via multimodal prompting," in *Proceedings of the IEEE/CVF Conference on Computer Vision and Pattern Recognition*, 2023, pp. 23 034–23 044.
- [13] B. Ni, H. Peng, M. Chen, S. Zhang, G. Meng, J. Fu, S. Xiang, and H. Ling, "Expanding language-image pretrained models for general video recognition," in *Computer Vision—ECCV 2022: 17th European Conference, Tel Aviv, Israel, October 23–27, 2022, Proceedings, Part IV*. Springer, 2022, pp. 1–18.
- [14] H. Rasheed, M. U. Khattak, M. Maaz, S. Khan, and F. S. Khan, "Fine-tuned clip models are efficient video learners," in *Proceedings of the IEEE/CVF Conference on Computer Vision and Pattern Recognition*, 2023, pp. 6545–6554.
- [15] R. Zhang, Z. Zeng, Z. Guo, and Y. Li, "Can language understand depth?" in *Proceedings of the 30th ACM International Conference on Multimedia*, 2022, pp. 6868–6874.
- [16] Y. Du, Z. Liu, J. Li, and W. X. Zhao, "A survey of vision-language pre-trained models," *arXiv preprint arXiv:2202.10936*, 2022.
- [17] F.-L. Chen, D.-Z. Zhang, M.-L. Han, X.-Y. Chen, J. Shi, S. Xu, and B. Xu, "Vlp: A survey on vision-language pre-training," *Machine Intelligence Research*, vol. 20, no. 1, pp. 38–56, 2023.
- [18] T. Mahmud and D. Marculescu, "Ave-clip: Audioclip-based multi-window temporal transformer for audio visual event localization," in *Proceedings of the IEEE/CVF Winter Conference on Applications of Computer Vision*, 2023, pp. 5158–5167.
- [19] R. Zhang, Z. Guo, W. Zhang, K. Li, X. Miao, B. Cui, Y. Qiao, P. Gao, and H. Li, "Pointclip: Point cloud understanding by clip," in *Proceedings of the IEEE/CVF Conference on Computer Vision and Pattern Recognition*, 2022, pp. 8552–8562.
- [20] Y. Zeng, C. Jiang, J. Mao, J. Han, C. Ye, Q. Huang, D.-Y. Yeung, Z. Yang, X. Liang, and H. Xu, "Clip2: Contrastive language-image-point pretraining from real-world point cloud data," in *Proceedings of the IEEE/CVF Conference on Computer Vision and Pattern Recognition*, 2023, pp. 15 244–15 253.
- [21] L. Xue, M. Gao, C. Xing, R. Martín-Martín, J. Wu, C. Xiong, R. Xu, J. C. Niebles, and S. Savarese, "Ulip: Learning a unified representation of language, images, and point clouds for 3d understanding," in *Proceedings of the IEEE/CVF Conference on Computer Vision and Pattern Recognition*, 2023, pp. 1179–1189.
- [22] X. Huang, S. Li, W. Qu, T. He, Y. Zuo, and W. Ouyang, "Frozen clip model is efficient point cloud backbone," *arXiv preprint arXiv:2212.04098*, 2022.

- [23] Z. Lin, S. Geng, R. Zhang, P. Gao, G. de Melo, X. Wang, J. Dai, Y. Qiao, and H. Li, "Frozen clip models are efficient video learners," in *European Conference on Computer Vision*. Springer, 2022, pp. 388–404.
- [24] M. Liu, Y. Zhu, H. Cai, S. Han, Z. Ling, F. Porikli, and H. Su, "Partslip: Low-shot part segmentation for 3d point clouds via pretrained image-language models," in *Proceedings of the IEEE/CVF Conference on Computer Vision and Pattern Recognition*, 2023, pp. 21 736–21 746.
- [25] K. Zhou, J. Yang, C. C. Loy, and Z. Liu, "Conditional prompt learning for vision-language models," in *Proceedings of the IEEE/CVF Conference on Computer Vision and Pattern Recognition*, 2022, pp. 16 816–16 825.
- [26] —, "Learning to prompt for vision-language models," *International Journal of Computer Vision*, vol. 130, no. 9, pp. 2337–2348, 2022.
- [27] H. Yao, R. Zhang, and C. Xu, "Visual-language prompt tuning with knowledge-guided context optimization," in *Proceedings of the IEEE/CVF Conference on Computer Vision and Pattern Recognition*, 2023, pp. 6757–6767.
- [28] M. Tsimpoukelli, J. L. Menick, S. Cabi, S. Eslami, O. Vinyals, and F. Hill, "Multimodal few-shot learning with frozen language models," *Advances in Neural Information Processing Systems*, vol. 34, pp. 200–212, 2021.
- [29] Z. Wang, J. Yu, A. W. Yu, Z. Dai, Y. Tsvetkov, and Y. Cao, "SimVlm: Simple visual language model pretraining with weak supervision," *arXiv preprint arXiv:2108.10904*, 2021.
- [30] S. Shen, S. Yang, T. Zhang, B. Zhai, J. E. Gonzalez, K. Keutzer, and T. Darrell, "Multitask vision-language prompt tuning," *arXiv preprint arXiv:2211.11720*, 2022.
- [31] D. Li, J. Li, H. Li, J. C. Niebles, and S. C. Hoi, "Align and prompt: Video-and-language pre-training with entity prompts," in *Proceedings of the IEEE/CVF Conference on Computer Vision and Pattern Recognition*, 2022, pp. 4953–4963.
- [32] J. Li, D. Li, S. Savarese, and S. Hoi, "Blip-2: Bootstrapping language-image pre-training with frozen image encoders and large language models," *arXiv preprint arXiv:2301.12597*, 2023.
- [33] M. Jia, L. Tang, B.-C. Chen, C. Cardie, S. Belongie, B. Hariharan, and S.-N. Lim, "Visual prompt tuning," in *European Conference on Computer Vision*. Springer, 2022, pp. 709–727.
- [34] H. Bahng, A. Jahanian, S. Sankaranarayanan, and P. Isola, "Exploring visual prompts for adapting large-scale models," *arXiv preprint arXiv:2203.17274*, 2022.
- [35] A. Bar, Y. Gandelsman, T. Darrell, A. Globerson, and A. Efros, "Visual prompting via image inpainting," *Advances in Neural Information Processing Systems*, vol. 35, pp. 25 005–25 017, 2022.
- [36] Y. Zang, W. Li, K. Zhou, C. Huang, and C. C. Loy, "Unified vision and language prompt learning," *arXiv preprint arXiv:2210.07225*, 2022.
- [37] R. Herzig, O. Abramovich, E. Ben-Avraham, A. Arbelle, L. Karlinsky, A. Shamir, T. Darrell, and A. Globerson, "Promptonomyvit: Multi-task prompt learning improves video transformers using synthetic scene data," *arXiv preprint arXiv:2212.04821*, 2022.
- [38] Y. Bai, C. Wang, S. Xie, C. Dong, C. Yuan, and Z. Wang, "Textir: A simple framework for text-based editable image restoration," *arXiv preprint arXiv:2302.14736*, 2023.
- [39] X. Li, X. Yin, C. Li, P. Zhang, X. Hu, L. Zhang, L. Wang, H. Hu, L. Dong, F. Wei *et al.*, "Oscar: Object-semantics aligned pre-training for vision-language tasks," in *Computer Vision—ECCV 2020: 16th European Conference, Glasgow, UK, August 23–28, 2020, Proceedings, Part XXX 16*. Springer, 2020, pp. 121–137.
- [40] Y. Yao, A. Zhang, Z. Zhang, Z. Liu, T.-S. Chua, and M. Sun, "Cpt: Colorful prompt tuning for pre-trained vision-language models," *arXiv preprint arXiv:2109.11797*, 2021.
- [41] J. Wang, P. Zhou, M. Z. Shou, and S. Yan, "Position-guided text prompt for vision-language pre-training," in *Proceedings of the IEEE/CVF Conference on Computer Vision and Pattern Recognition*, 2023, pp. 23 242–23 251.
- [42] A. Kirillov, E. Mintun, N. Ravi, H. Mao, C. Rolland, L. Gustafson, T. Xiao, S. Whitehead, A. C. Berg, W.-Y. Lo *et al.*, "Segment anything," *arXiv preprint arXiv:2304.02643*, 2023.
- [43] A. Sironi, M. Brambilla, N. Bourdis, X. Lagorce, and R. Benosman, "HATS: Histograms of averaged time surfaces for robust event-based object classification," in *CVPR*, 2018.
- [44] R. W. Baldwin, M. Almatrafi, J. R. Kaufman, V. Asari, and K. Hirakawa, "Inceptive event time-surfaces for object classification using neuromorphic cameras," in *ICIAR*, 2019.
- [45] D. Gehrig, A. Loquercio, K. G. Derpanis, and D. Scaramuzza, "End-to-end learning of representations for asynchronous event-based data," in *ICCV*, 2019.
- [46] J. Botzheim, T. Obo, and N. Kubota, "Human gesture recognition for robot partners by spiking neural network and classification learning," in *SCIS*, 2012.
- [47] A. Amir, B. Taba, D. Berg, T. Melano, J. McKinstry, C. Di Nolfo, T. Nayak, A. Andreopoulos, G. Garreau, M. Mendoza *et al.*, "A low power, fully event-based gesture recognition system," in *CVPR*, 2017.
- [48] Y. Deng, H. Chen, H. Liu, and Y. Li, "A Voxel Graph CNN for Object Classification With Event Cameras," in *CVPR*, 2022.
- [49] A. Dosovitskiy, L. Beyer, A. Kolesnikov, D. Weissenborn, X. Zhai, T. Unterthiner, M. Dehghani, M. Minderer, G. Heigold, S. Gelly *et al.*, "An image is worth 16x16 words: Transformers for image recognition at scale," *arXiv preprint arXiv:2010.11929*, 2020.
- [50] K. He, X. Zhang, S. Ren, and J. Sun, "Deep residual learning for image recognition," in *Proceedings of the IEEE conference on computer vision and pattern recognition*, 2016, pp. 770–778.
- [51] A. Vaswani, N. Shazeer, N. Parmar, J. Uszkoreit, L. Jones, A. N. Gomez, Ł. Kaiser, and I. Polosukhin, "Attention is all you need," *Advances in neural information processing systems*, vol. 30, 2017.
- [52] J. L. Ba, J. R. Kiros, and G. E. Hinton, "Layer normalization," *arXiv preprint arXiv:1607.06450*, 2016.
- [53] S. Schaefer, D. Gehrig, and D. Scaramuzza, "Aegnn: Asynchronous event-based graph neural networks," in *Proceedings of the IEEE/CVF conference on computer vision and pattern recognition*, 2022, pp. 12 371–12 381.
- [54] N. Messikommer, D. Gehrig, A. Loquercio, and D. Scaramuzza, "Event-based asynchronous sparse convolutional networks," in *Computer Vision—ECCV 2020: 16th European Conference, Glasgow, UK, August 23–28, 2020, Proceedings, Part VIII 16*. Springer, 2020, pp. 415–431.
- [55] Y. Bi, A. Chadha, A. Abbas, E. Boursoulatze, and Y. Andreopoulos, "Graph-based object classification for neuromorphic vision sensing," in *Proceedings of the IEEE/CVF international conference on computer vision*, 2019, pp. 491–501.
- [56] Z. Wang, Y. Hu, and S.-C. Liu, "Exploiting spatial sparsity for event cameras with visual transformers," in *2022 IEEE International Conference on Image Processing (ICIP)*. IEEE, 2022, pp. 411–415.
- [57] M. Cannici, M. Ciccone, A. Romanoni, and M. Matteucci, "A differentiable recurrent surface for asynchronous event-based data," in *Computer Vision—ECCV 2020: 16th European Conference, Glasgow, UK, August 23–28, 2020, Proceedings, Part XX 16*. Springer, 2020, pp. 136–152.
- [58] H. Rebecq, R. Ranftl, V. Koltun, and D. Scaramuzza, "Events-to-video: Bringing modern computer vision to event cameras," in *Proceedings of the IEEE/CVF Conference on Computer Vision and Pattern Recognition*, 2019, pp. 3857–3866.
- [59] F. Gu, W. Sng, X. Hu, and F. Yu, "Eventdrop: Data augmentation for event-based learning," *arXiv preprint arXiv:2106.05836*, 2021.
- [60] J. Deng, W. Dong, R. Socher, L.-J. Li, K. Li, and L. Fei-Fei, "Imagenet: A large-scale hierarchical image database," in *2009 IEEE conference on computer vision and pattern recognition*. Ieee, 2009, pp. 248–255.
- [61] L. Fei-Fei, R. Fergus, and P. Perona, "Learning generative visual models from few training examples: An incremental bayesian approach tested on 101 object categories," in *2004 conference on computer vision and pattern recognition workshop*. IEEE, 2004, pp. 178–178.
- [62] G. Orchard, A. Jayawant, G. K. Cohen, and N. Thakor, "Converting static image datasets to spiking neuromorphic datasets using saccades," *Frontiers in neuroscience*, vol. 9, p. 437, 2015.
- [63] L. Deng, "The mnist database of handwritten digit images for machine learning research [best of the web]," *IEEE signal processing magazine*, vol. 29, no. 6, pp. 141–142, 2012.
- [64] C. Posch, D. Matolin, and R. Wohlgenannt, "A qvga 143 db dynamic range frame-free pwm image sensor with lossless pixel-level video compression and time-domain cds," *IEEE Journal of Solid-State Circuits*, vol. 46, no. 1, pp. 259–275, 2010.
- [65] A. Dosovitskiy, L. Beyer, A. Kolesnikov, D. Weissenborn, X. Zhai, T. Unterthiner, M. Dehghani, M. Minderer, G. Heigold, S. Gelly *et al.*, "An image is worth 16x16 words: Transformers for image recognition at scale. arxiv 2020," *arXiv preprint arXiv:2010.11929*, 2010.
- [66] A. Paszke, S. Gross, F. Massa, A. Lerer, J. Bradbury, G. Chanan, T. Killeen, Z. Lin, N. Gimelshein, L. Antiga *et al.*, "Pytorch: An imperative style, high-performance deep learning library," *Advances in neural information processing systems*, vol. 32, 2019.
- [67] D. P. Kingma and J. Ba, "Adam: A method for stochastic optimization," *arXiv preprint arXiv:1412.6980*, 2014.
- [68] I. Loshchilov and F. Hutter, "Sgdr: Stochastic gradient descent with warm restarts," *arXiv preprint arXiv:1608.03983*, 2016.
- [69] Y. Yang, L. Pan, and L. Liu, "Event camera data pre-training," *arXiv preprint arXiv:2301.01928*, 2023.

- [70] S. Klenk, D. Bonello, L. Koestler, and D. Cremers, “Masked event modeling: Self-supervised pretraining for event cameras,” *arXiv preprint arXiv:2212.10368*, 2022.
- [71] P. Young, A. Lai, M. Hodosh, and J. Hockenmaier, “From image descriptions to visual denotations: New similarity metrics for semantic inference over event descriptions,” *Transactions of the Association for Computational Linguistics*, vol. 2, pp. 67–78, 2014.
- [72] X. Chen, H. Fang, T.-Y. Lin, R. Vedantam, S. Gupta, P. Dollár, and C. L. Zitnick, “Microsoft coco captions: Data collection and evaluation server,” *arXiv preprint arXiv:1504.00325*, 2015.



Zhou Jiazhou is a research assistant in the Visual Learning and Intelligent Systems Lab, Artificial Intelligence Thrust, The Hong Kong University of Science and Technology, Guangzhou (HKUST-GZ). Her research interests include event-based vision, multi-modal learning, *etc.*



Xu Zheng (IEEE Student Member) is a Ph.D. student in the Visual Learning and Intelligent Systems Lab, Artificial Intelligence Thrust, The Hong Kong University of Science and Technology, Guangzhou (HKUST-GZ). His research interests include event-based vision, 3D vision, *etc.*



Yuanhuiyi Lyu is a research assistant in the Visual Learning and Intelligent Systems Lab, Artificial Intelligence Thrust, The Hong Kong University of Science and Technology, Guangzhou (HKUST-GZ). His research interests include event-based vision, multi-modal learning, natural language processing, *etc.*



Lin Wang (IEEE Member) is an assistant professor in the AI Thrust, HKUST-GZ, and an affiliate assistant professor in the Dept. of CSE, HKUST. He did his Postdoc at the Korea Advanced Institute of Science and Technology (KAIST). He got his Ph.D. (with honors) and M.S. from KAIST, Korea. He had rich cross-disciplinary research experience, covering mechanical, industrial, and computer engineering. His research interests lie in computer and robotic vision, machine learning, intelligent systems (XR, vision for HCI), *etc.*

For more about me, please visit <https://vlislab22.github.io/vlislab/>.

E-CLIP: Towards Label-efficient Event-based Open-world Understanding by CLIP

–Supplementary Material–

Jiazhou Zhou*, Xu Zheng*, *Student Member, IEEE*, Yuanhuiyi Lyu, Lin Wang†, *Member, IEEE*
Project homepage: <https://vlislab22.github.io/ECLIP/>



APPENDIX

1 IMPLEMENTATION DETAILS

1.1 Event Representation

Event cameras capture object movement by detecting temporal independence and recording pixel-level brightness changes. The event stream, denoted as $\mathcal{E} = e_i(x_i, y_i, t_i, p_i)$, reflects the brightness change e_i of a pixel at the timestamp t_i , with coordinates (x_i, y_i) , and polarity $p_i \in \{1, -1\}$. Here, 1 and -1 represent the positive and negative intensity change of brightness, respectively.

To obtain a grid-like tensor as the input, we convert the event stream into a sequence of frames. First, we normalize the length of the event stream \mathcal{E} to a fixed amount P using zero-padding or taking the first P events. Then, we group every Q consecutive event data in the normalized event stream \mathcal{E}' to obtain event parts $\mathcal{E}'' \in \mathbb{R}^{T \times 4 \times P}$, where $T = P/Q$ and denotes the number of event frames. We then transform these event parts into histograms $h \in \mathbb{R}^{T \times H \times W \times 2}$ by counting the amount of positive and negative events per pixel, where H and W represent the height and width of an event frame, respectively. Finally, to attain the grid-like 3-channel input $I_e \in \mathbb{R}^{T \times H \times W \times 3}$, we colorize the t th event histogram h_t by multiplying the predefined red color map $[0, 255, 255]$ and blue color map $[255, 255, 0]$ with the positive and negative event histogram respectively and merge them by pixel-wise addition, which can be formulated as follow:

$$I_{e,t} = h_t^p [0, 255, 255]^T + h_t^n [255, 255, 0]^T, \quad (1)$$

where the $I_{e,t}$ represents the event input for the t th event frame and $t = 0, 1, \dots, T$; h_t^p and h_t^n denotes the positive and negative event histogram respectively. Finally, the generated event frame input is resized into the 224×224 resolution for adapting to the ViT setting, generating the final event input $I'_e \in \mathbb{R}^{T \times 224 \times 224 \times 3}$.

The above grid-like event representation is simple yet effective since the generated event image resembles the edge image, whose

- J. Zhou, X. Zheng, Y. Lyu are with the AI Thrust, HKUST(GZ), Guangzhou, China. E-mail: zhengxu128@gmail.com, {jiazhouzhou, yuanhuiyilyu}@kust-gz.edu.cn
- L. Wang is with the AI Thrust, HKUST(GZ), Guangzhou, and Dept. of Computer Science and Engineering, HKUST, Hong Kong SAR, China. E-mail: linwang@ust.hk

Manuscript received April 19, 2022; revised August 26, 2022.

(* Equal contribution, † Corresponding author: Lin Wang)

Length of text learnable prompt	Top1 Accuracy	
	N-Caltech101	N-MNIST
4	92.50	97.20
8	92.68	98.50
16	92.92	98.71

TABLE 1
Ablation study on the length of text learnable prompt.

Length of event modality prompt	Top1 Accuracy	
	N-Caltech101	N-MNIST
4	92.50	97.75
8	92.68	98.73
16	92.92	98.82

TABLE 2
Ablation study on the length of event modality prompts

data distribution is much closer to the pre-trained natural images so that the transfer pressure is erased and the modality gap is bridged.

2 ADDITIONAL EXPERIMENT RESULT

2.1 Accuracy Curve

Two significant ablation experiments conducted on the N-Caltech101 dataset of E-CLIP are chosen for analysis. These investigations include an ablation study that explores various combinations of the proposed module, as well as an ablation study that investigates the Hierarchical Triple Contrastive Alignment (HTCA) module. We present the loss curves of them in Fig. 1 to observe their accuracy change with varying ablation settings. As shown in Fig. 1, the accuracy of the model exhibits fluctuations that tend to rise as the number of training epochs increases. The observed discrepancy in the ultimate accuracy across several ablation versions of the model provides more evidence supporting the efficacy and logicity of the proposed model.

2.2 Visualization of Few-shot Event Recognition Results

Fig. 2 displays the accuracy curve with different evaluation settings, including zero-shot, few-shot, and fine-tuning on the N-Caltech101, NMIST, and N-Imagenet datasets respectively. We conduct a comparative analysis between E-CLIP and the existing EventCLIP on the N-Caltech101 and N-ImageNet datasets. Our findings indicate that E-CLIP outperforms its competition when provided with a minimum of five training examples. These results highlight the efficacy and label efficiency of the E-CLIP model.

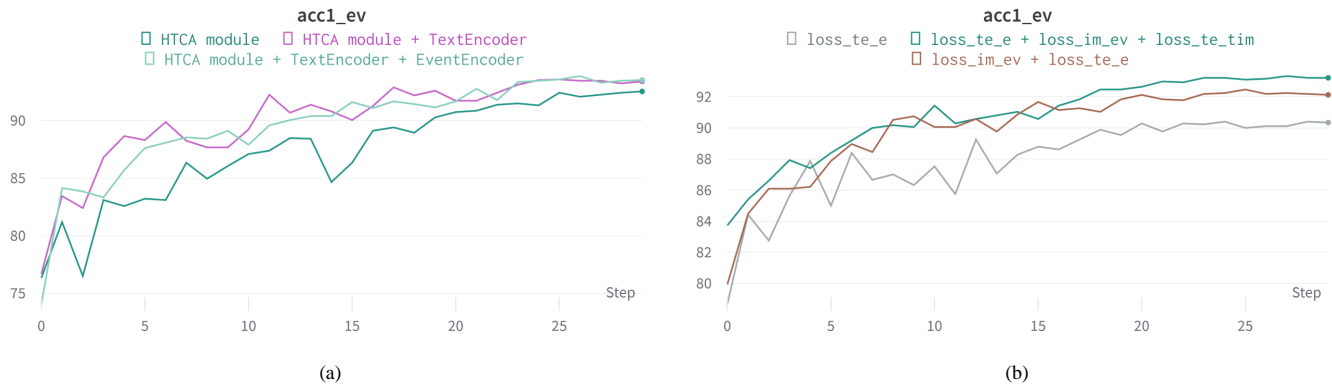


Fig. 1. Visualization of accuracy curve on two selected important ablation studies on the N-Caltech101 dataset of our proposed E-CLIP. (a) The ablation study on different combinations of the proposed module; (b) The ablation study on the HTCA module.

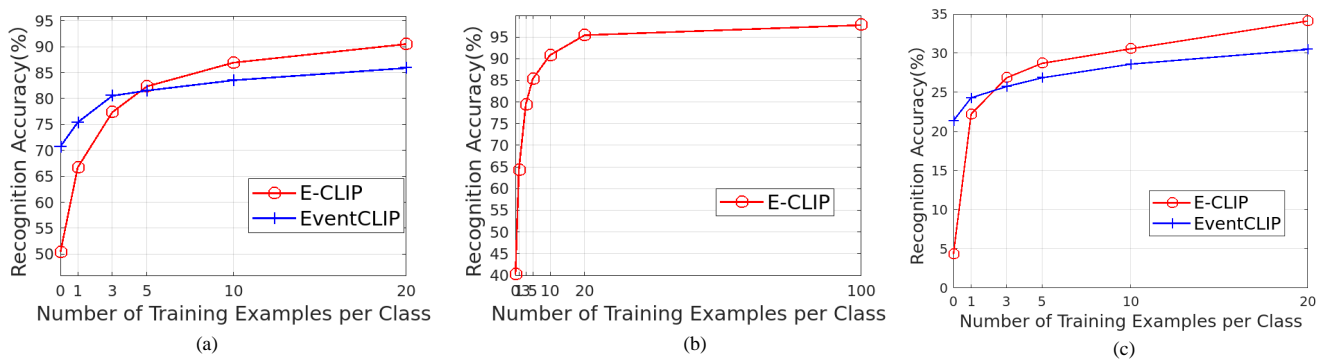


Fig. 2. Visualization of event recognition results with zero-shot, few-shot settings. (a) Results on the N-Caltech101 dataset; (b) Results on the NMIST dataset; (c) Results on the N-Imagenet dataset.

Setting	Text2Event			Image2Event		
	Recall@1	Recall@5	Recall@10	Recall@1	Recall@5	Recall@10
0-shot	78.22	88.12	91.09	79.40	90.34	93.58
1-shot	81.19	95.05	98.02	82.75	96.04	99.01
2-shot	90.10	99.01	100.00	88.31	98.02	99.01
5-shot	97.03	100.00	100.00	90.97	99.01	100.00
10-shot	98.02	100.00	100.00	94.73	99.01	100.00
20-shot	99.01	100.00	100.00	96.70	100.00	100.00
Fine-tune	100.00	100.00	100.00	96.88	99.60	99.95

TABLE 3

Event Retrieval results on N-Caltech101 dataset with zero-shot, few-shot, and fine-tuning settings.

2.3 Full Numerical Results

In the main paper, we plot E-CLIP’s ablation study on the length of the text learnable prompts, ablation study on the length of the event modality prompts, and Event retrieval results on N-Caltech101 dataset with zero-shot, few-shot, and fine-tuning settings in Fig. 7(a), Fig. 7(b) and Fig. 9 respectively. To ease future comparison, we report all those numbers in Tab. 1, Tab. 2, and Tab. 3.